# Development of Metastatic and Non-Metastatic Tumor Lines From a Patient's Prostate Cancer Specimen—Identification of a Small Subpopulation With Metastatic Potential in the Primary Tumor

Dong Lin,[1] Jane Bayani,[2] Yuwei Wang,[1] Marianne D. Sadar,[3] Maisa Yoshimoto,[4] Peter W. Gout,[1] Jeremy A. Squire,[4] and Yuzhuo Wang[1,5,6]*

[1]Department of Cancer Endocrinology, BC Cancer Agency, Vancouver, BC, Canada
[2]Department of Laboratory Medicine and Pathobiology, University of Toronto, Toronto, ON, Canada
[3]Department of Genome Sciences Centre, BC Cancer Agency, Vancouver, BC, Canada
[4]Department of Pathology and Molecular Medicine, Queen's University and Kingston General Hospital, Kingston, ON, Canada
[5]Department of Urologic Sciences, University of British Columbia, Vancouver, BC, Canada
[6]The Living Tumor Laboratory at the Vancouver Prostate Centre, Vancouver, BC, Canada

**BACKGROUND.** Metastasis is the major cause of prostate cancer deaths. Tumor heterogeneity in both primary and metastatic prostate cancers is a major hurdle in elucidating the mechanisms of metastasis in this disease. To circumvent this obstacle and improve our understanding of prostate cancer metastasis, we developed multiple tumor tissue lines from one patient's primary prostate cancer specimen to examine differences in metastatic ability.
**METHODS.** Pieces of tissue from different foci of a patient's primary prostate tumor were grafted into subrenal capsules of NOD-SCID mice and transplantable tumor sublines were established by serial passage. The metastatic ability of each subline was tested via orthotopic grafting into mice. Chromosomal alterations exclusively presented in a metastatic subline were examined by SKY and investigated for their presence in parental tissues by fluorescence in situ hybridization.
**RESULTS.** Three transplantable sublines were developed, resembling the primary tumor histologically, exhibiting poor differentiation, and different growth rates. Importantly, the LTL-220N and LTL-221N sublines were non-metastatic, whereas the LTL-220M subline was spontaneously metastatic in vivo. SKY analysis showed limited but unique chromosomal alterations in each subline. Some chromosomal alterations, exclusively present in the metastatic LTL-220M subline, were also observed in a small portion of the parental cancer tissues.
**CONCLUSION.** The results indicate that in primary prostate tumors metastatic potential can be confined to a minority of cancer cells. Subrenal capsule xenograft methodology can be used to dissect heterogeneous cancer cells in a patient's primary tumor and sublines derived from such cells provide valuable tools for investigating mechanisms underlying prostate cancer metastasis. *Prostate 70: 1636–1644, 2010.* © 2010 Wiley-Liss, Inc.

KEY WORDS: prostate cancer; metastasis; xenograft; FISH

## INTRODUCTION

The majority of prostate cancer deaths is caused by metastatic dissemination of the primary tumor [1]. Metastasis is a complex multi-step process thought to be driven by changes in the expression of multiple genes caused by genetic or/and epigenetic alterations [2,3]. Prostate cancer has been recognized as a multi-focal disease that generally consists of a dominant cancer and one or more independent cancers of smaller volume with different histological features and a wide spectrum of biological behavior [4–7]. The histological, biological, and genetic heterogeneity of multifocal prostate cancers suggests that they arise independently from different clones [8–11]. Experimental assays based on a mouse cancer cell line demonstrated that only a small portion of cancer cells were endowed with metastasis-promoting functions, indicating that metastatic lesions are derived from descendants of a rare cell in the primary tumor [11]. On the other hand, advances in molecular profiling of cancers suggest that the metastatic potential of human tumors is encoded in the bulk of a primary tumor, thus challenging the above hypothesis [12]. It is still controversial as to whether a minority or a majority of cancer cells in primary tumors has metastatic potential.

Studies of prostate cancer metastasis at the cellular and tissue levels have been impeded by a lack of optimal experimental models. While established cultured cancer cell lines representing different stages of cancer progression can be very useful for identifying mechanisms underlying metastasis, they do not adequately mimic clinical disease [13,14]. Efforts have therefore focused on use of prostate cancer specimens from patients. However, the significant differences in microenvironment between primary and secondary prostate cancers and the typical heterogeneity of such specimens (e.g., consisting of both non-metastatic and potentially metastatic subpopulations) make it difficult to identify genes underlying the development of metastasis [15]. To overcome the above hurdles, we recently developed experimental prostate cancer models that resemble the clinical situation and allow establishment of transplantable prostate cancer sublines that differ in metastatic ability and as such can be useful for investigating development of metastasis at the cellular and molecular levels. The model is based on subrenal capsule grafting of pieces of a patient's primary prostate cancer tissue into immuno-deficient mice leading to establishment of multiple transplantable tumor lines retaining major growth and histopathological features of the original cancer [16–19].

The present study was aimed at establishing tumor lines with different metastatic ability from a patient's primary prostate cancer and examining whether metastatic potential of the disease is associated with a minority of the cells in a primary tumor or with the bulk of the tumor. To achieve this, a number of transplantable prostate cancer sublines were developed via subrenal capsule grafting in NOD-SCID mice from different foci of a prostate cancer. Tissue invasive or metastatic abilities of the sublines were then determined in vivo via orthotopic grafting and monitoring organs/tissues of the hosts. Each subline was then investigated for chromosomal alterations. Such alterations, exclusively present in a metastatic subline, were further investigated in parental cancer tissues by fluorescence in situ hybridization (FISH) to identify the cells in the primary tumor which carried the same chromosomal alterations.

## MATERIALS AND METHODS

### Materials and Animals

Chemicals, stains, solvents, and solutions were obtained from Sigma–Aldrich Canada Ltd (Oakville, ON, Canada), unless otherwise indicated. Male 6- to 8-week-old NOD-SCID mice were bred by the BC Cancer Research Centre Animal Resource Centre (BC Cancer Agency, Vancouver, Canada). Mice were housed in groups of three in microisolators with free access to food and water and their health was monitored daily. Animal care and experiments were carried out in accordance with the guidelines of the Canadian Council on Animal Care.

### Prostate Cancer Tissue Acquisition

Prostate cancer tissue specimens were obtained via prostatectomy from a 70-year-old male, with informed consent, at the Urology Research Unit (Carlton Centre, San Fernando, Trinidad). The patient was diagnosed with advanced prostate cancer (Gleason grade $5+5$) and had not received neoadjuvant therapy. No detectable metastasis was observed prior to prostatectomy. The specimens obtained from different foci were examined independently and confirmed to have the same histopathological grade by pathologists. The samples were shipped overnight, immersed in cold Hanks' balanced salt solution supplemented with antibiotics, to Vancouver (Canada).

### Subrenal Capsule Grafting and Development of Transplantable Tumor Tissue Lines

Xenografting was performed as previously described [16]. In brief, within 24 hr of its arrival, tumor tissue was cut into small pieces about $1 \times 3 \times 3 \, mm^3$ in size. The tumor pieces were grafted under the kidney capsules of male NOD-SCID mice supplemented with

testosterone (10 mg/mouse) via subcutaneously implanted testosterone pellets. After 90 days of growth (or earlier if required by the health status of the hosts), the animals were sacrificed by $CO_2$ for necropsy. Tumors were harvested, measured, photographed, and fixed for histopathological analysis. Some of the rapidly growing tumors were cut into pieces and maintained for up to five transplant generations by serial subrenal capsule transplantation into testosterone-supplemented male NOD-SCID mice. Three patients derived transplantable tumor lines from generations 10–13 were used for this study.

### In Vivo Orthotopic Metastatic Assay

Orthotopic grafting was performed as previously described [16]. In brief, tumor tissues were harvested and then grafted into the anterior prostates of male, testosterone-supplemented NOD-SCID mice (two per mouse). After 5 weeks, mice were sacrificed for gross examination of lymph nodes. Lymph nodes, lungs, livers, kidneys, spleens, and bone (femur) of the hosts were fixed for examination of metastases using histological and immunohistochemical techniques.

### Histopathological and Immunohistochemical Staining

Tissues of the original tumor specimen, its transplants and metastases were fixed in 10% neutral buffered formalin and then embedded in paraffin. Sections (5 µm thick) were cut on a microtome and mounted on glass slides. For histopathological examination, every fourth section was de-waxed in Histoclear (National Diagnostic, Atlanta, GA) and hydrated in graded alcohol solutions and distilled water for H&E staining and examination under a light microscope. For immunohistochemical staining, endogenous peroxidase activity was blocked with 0.5% hydrogen peroxide in methanol for 30 min followed by washing in phosphate buffered saline (PBS), pH 7.4. Five percent normal goat serum in PBS was applied to the sections for 30 min to block non-specific sites. The sections were then incubated with primary antibodies overnight at 4°C or with control IgG from non-immunized mice or rabbits. Mouse anti-human mitochondria monoclonal antibody was obtained from Chemicon International (Temecula, CA), rabbit anti-human PTEN monoclonal antibody was purchased from Cell Signaling Technologies (Danvers, MA). Following incubation with the primary antibodies, sections were washed with PBS and incubated for 30 min at room temperature with biotinylated secondary anti-mouse secondary antibody (Amersham International, Arlington Heights, IL). After incubation with the secondary antibodies, sections were washed in PBS (three 10-min washes), and then

incubated for 30 min at room temperature with avidin–biotin complex (Vector Laboratories, Burlingame, CA). Following a further 30 min of washing in PBS, immunoreactivity was visualized using 3,3'-diaminobenzidine tetrahydrochloride (DAB) in PBS and 0.03% hydrogen peroxide. Sections were counterstained with 5% (w/v) Harris hematoxylin and dehydrated in graded alcohols. Control sections were processed in parallel with rabbit non-immune IgG (Dako, Carpinteria, CA) used at the same concentrations as the primary antibodies.

### Spectral Karyotyping

Standard metaphase spreads were prepared from actively growing xenograft cultures as previously described [19,20]. The slides were hybridized with SKYPaints (Applied Specrtral Imaging Inc. Vista, CA) according to the manufacturer's instructions. The hybridized slides were imaged and analyzed using Applied Spectral Imaging HiSKY analysis software (ASI Inc.).

### Fluorescence In Situ Hybridization (FISH)

For copy number analysis, a bacterial artificial chromosome (BAC) clone RP11-464P23, covering *FBXO9* (6p12), was obtained from The Centre for Applied Genomics (TCAG, Toronto, Canada). DNA was extracted from this BAC clone and directly labeled with Spectrum Green dUPT (Vysis/Abbott Laboratories, Des Plaines, IL) by nick translation, using the Vysis Nick Translation Kit (Vysis/Abbott Laboratories). To confirm the proper mapping location and hybridization efficiency, the labeled BAC clone was hybridized to normal human metaphase spreads. A SpectrumOrange labeled probe for *PTEN* was obtained from Vysis (Vysis/Abbott Laboratories) as well as a SpectrumAqua labeled centromere 6 probe (Vysis/Abbott Laboratories). Formalin-fixed, paraffin-embedded (FFPE) tissue sections (5 µm thick), representing early xenografts derived from individual tumor foci and subsequently derived sublines, were dewaxed in xylene and dehydrated in 100% ethanol. The tissue sections were incubated in 10 mM citrate buffer at 80°C for 1 hr, rinsed in water, pepsin digested and dehydrated, and co-denatured for 10 min at 80°C using the Vysis Hybrite Hybridization System (Vysis/Abbott Laboratories) and then allowed to hybridize overnight at 37°C. The following day, the slides were processed using a wash of 0.3% NP-40/0.4× SSC for 2 min at 72°C and a wash of 0.1%NP-40/2× SSC for 5 min at RT. The slides were rinsed in 1× PBS and mounted with DAPI/Antifade medium (Vectashield/Vector Laboratories, Canada). Two hundred nuclei per slide were scored using a fluorescence microscope (Carl Zeiss, Canada)

and cut-off values for copy-number changes derived from the scoring of normal prostate cells as previously described by Yoshimoto et al. [21].

## RESULTS

### Development of Metastatic and Non-Metastatic Sublines From Primary Prostate Cancer Tissue Via Xenografting and In Vivo Metastatic Assay

The procedures for development of these sublines and assessing their metastatic ability are briefly illustrated in Figure 1. Tissues derived from different foci in a prostate cancer specimen from one patient were grafted under kidney capsules of NOD-SCID mice supplemented with testosterone and propagated by serial subrenal capsule grafting. Three tumor tissue lines were developed from parental tissues with tumor volume doubling times of 4, 4, and 7 days (Table I). All three lines were poorly differentiated and histologically similar to the parental tissues (Fig. 2A–C). The human origin of the tumor lines was confirmed by immunohistochemistry using anti-human mitochondria antibody (Fig. 2D–F). The metastatic ability of each tumor tissue line was determined by examination of tissues/organs of mice carrying xenografts in the orthotopic site (anterior prostate). At 6 weeks after grafting, apparent local tissue invasion was observed in mice carrying a tumor line designated LTL-220M (Fig. 2A,D). In addition, major metastatic foci were observed in local lymph nodes and distal metastases were found in lung, liver, kidney, and spleen (Fig. 2G,J). In contrast, the other tumor lines, that is, LTL-220N and LTL-221N, derived from different foci, did not show significant local tissue invasion or distal metastases (Fig. 2B,C,E,F,H,I,K,L, Table I).

### Identification by SKY of Unique Chromosomal Aberrations in Tumor Tissue Lines

SKY analysis was performed to identify unique chromosomal aberrations present in the metastatic tumor line but not in the two non-metastatic tumor lines. It was found that all three tumor lines were diploid in nature but had different chromosomal alterations (Fig. 3A–C). LTL-220M:46,XY,+der(1;14)(14p11→14q:1p11→1qter),del2p23,der(3)t(2;3)(?;p24),der(6)t(6,10)(p;q23),−14; LTL-220N:46,der(X)(X;16) (qter; p11),Y,der(21)?t(?;21)(?;p11); LTL-221N: 47,XY,der(14)t(13or18;14)(q?;p11),der(14)(6?;14)(?;qter),der(0)dup(20)(q13qter) t(4;20)(q22;qter),der(21)?t(?;21)(?:?). There was a marked difference between the metastatic LTL-220M and the non-metastatic LTL-220N and LTL-221N tumor lines in a net gain of 10q and net loss of 6p.
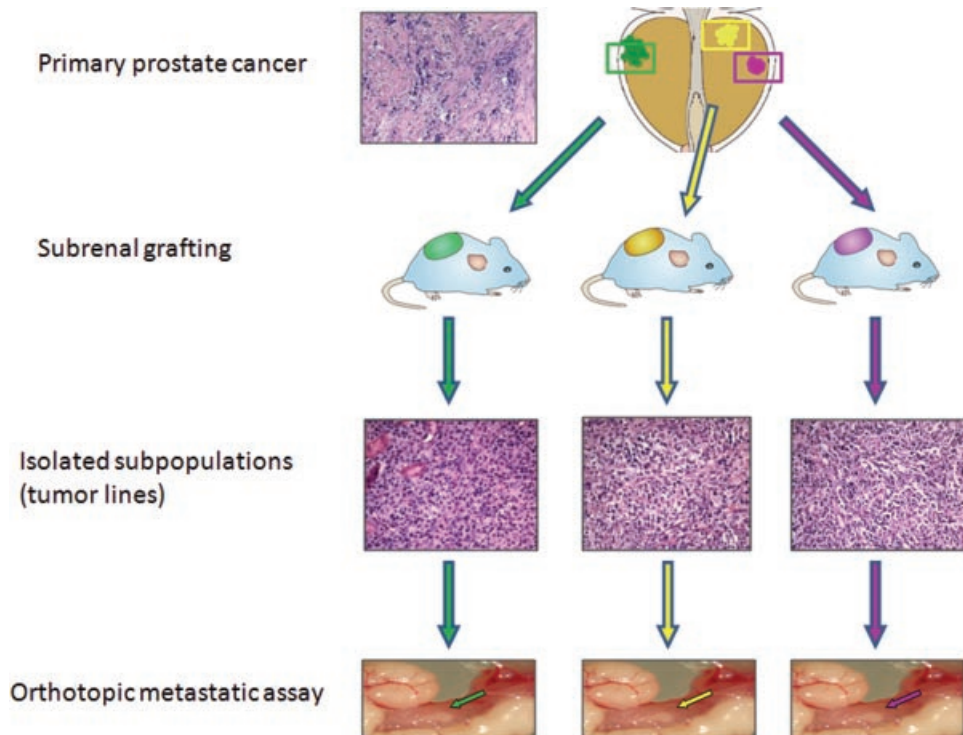


**Fig. I.** Development of metastatic and non-metastatic tumor tissue sublines from a primary prostate cancer tissue. H&E staining show the similar histological morphology between parental tissue and developed tumor lines. Arrows show the tumor tissues grafted in the prostates of NOD-SCID mice. [Color figure can be viewed in the online issue, which is available at wileyonlinelibrary.com.]

**TABLE I. Biological Characteristics of Tumor Lines LTL-220M, LTL-220N, and LTL-22IN**

|  | LTL-220M | LTL-220N | LTL-221N |
|---|---|---|---|
| Doubling time | 4 days | 4 days | 7 days |
| Local invasion | Yes | Yes/no | No |
| Local lymph node metastasis | Yes | No | No |
| Distal metastasis | Yes | No | No |

Based on the SKY data, the gain of 10q22.1–10qter and loss of 6p can in this case be used as a signature for distinguishing metastatic populations from non-metastatic populations.

## Detection of Cancer Cells Carrying the Metastatic Clone Signature (10q and 6p Alterations) in Parental Tissues

To determine the presence of the 10q and 6p alterations previously identified by SKY, the three tumor tissue lines were examined by FISH, using a SpectrumGreen-labeled probe for *FBXO9* (6p12), SpectrumAqua-labeled probe for centromere 6, and a SpectrumOrange-labeled probe for *PTEN* (10q23). As expected, FISH identified two copies for *PTEN* (10q23), centromere 6, and *FBXO9* (6p12) per cell in both the LTL-220N and LTL-221N non-metastatic tumor lines (Fig. 4B,C). The metastatic LTL-220M tumor line showed an overall net loss of *FBXO9* (6p12) and gain of *PTEN* (10q23). This net change, however, was the
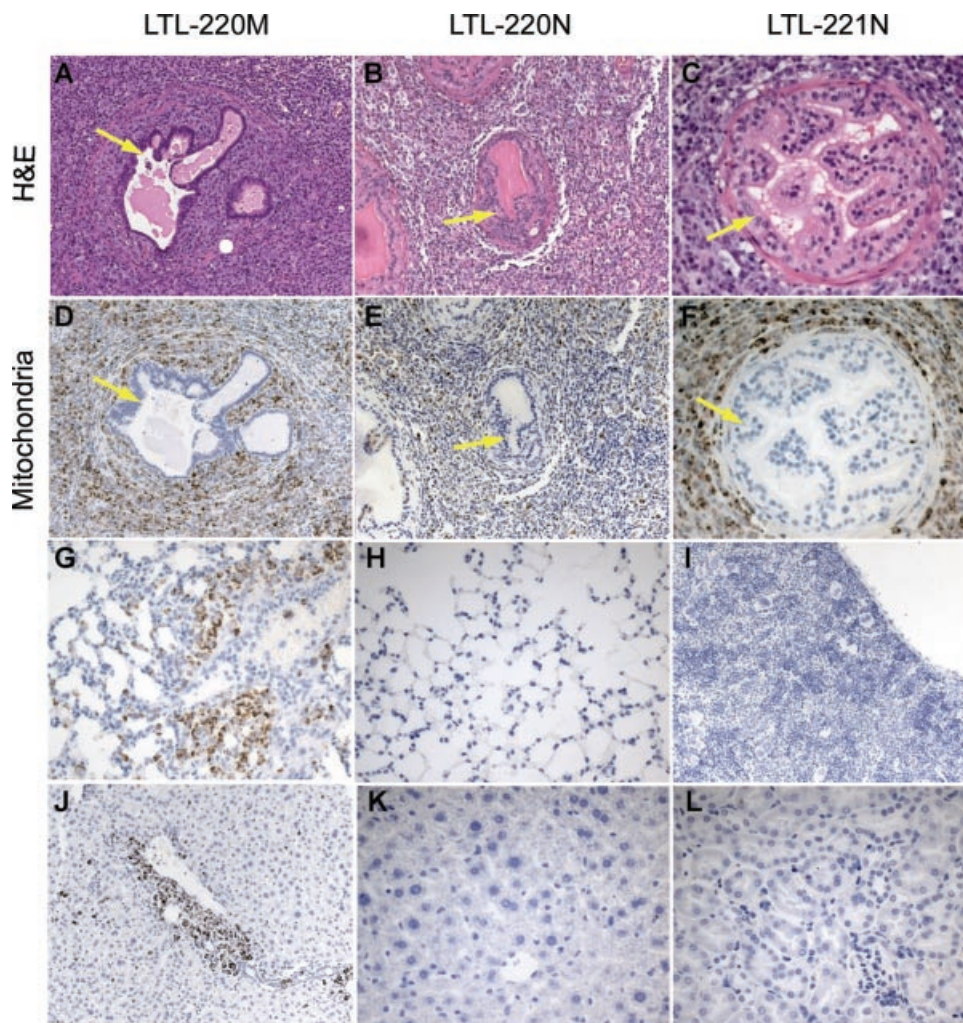


**Fig. 2.** Different local invasive and metastatic abilities of the LTL-220M, LTL-220N, and LTL-22IN sublines. **A–C**: Hematoxylin and eosin (H&E) staining. **D–L**: Immunohistochemical staining with human-specific anti-mitochondria antibody. Column I: when grafted orthotopically, the LTL-220M showed extensive invasion into host prostate (A,D) and distant metastases to host lung (G) and liver (J). Column 2 and 3: when grafted orthotopically, the LTL-220N and LTL-22IN did not show apparent invasion to host prostate and no metastasis to distant organs including lung (H), spleen (I), liver (K), and kidney (L). Mouse prostate are indicated with arrows. (Original magnification: A, B, D, E, G–J ×200; C, F, K, L ×400.) [Color figure can be viewed in the online issue, which is available at wileyonlinelibrary.com.]
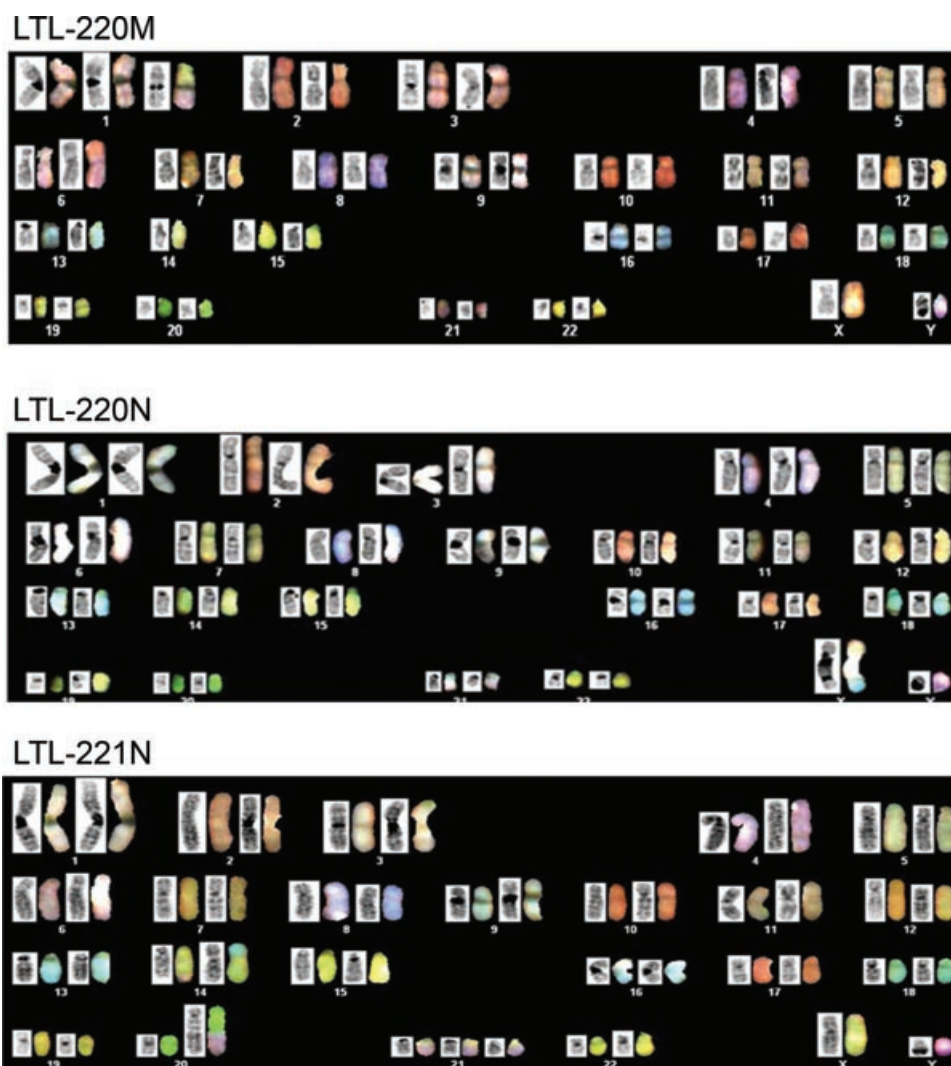
**Fig. 3.** SKY analysis of the LTL-220M, LTL-220N, and LTL-221N sublines. The metastatic LTL-220M (**A**) showed the primary clone with an unbalanced translocation der(6)t(6,10)(p;q23) resulting in the net loss of 6p and gain of 10q. The non-metastatic LTL-220N (**B**) and LTL-221N (**C**) showed no changes in copy number of chromosomes 6 or 10, but aberrations of other chromosomes. [Color figure can be viewed in the online issue, which is available at wileyonlinelibrary.com.]

result of three different subpopulations of similar frequency, which were identified by FISH showing similar chromosome alterations: (i) a gain of *PTEN* (10q23), loss of *FBXO9* (6p12), two copies of centromere 6; (ii) a gain of *PTEN* (10q23), three copies of centromere 6, and two copies of *FBXO9* (6p12); (iii) a gain of *PTEN*, two copies of centromere 6 and one copy of *FBXO9* (6p12) (Fig. 4A). Thus, the net gain for *PTEN* was typically due to the gain of one to two additional copies, in conjunction with the three copies in the stemline. For *FBXO9* (6p12), the majority of the cells only showed one copy for the locus (~60%), but in cells where there were two copies for *FBXO9* (6p12), there was a concomitant extra copy of centromere 6. Thus, the two copies of *FBXO9* (6p12) were likely a result of polysomy for normal chromosome 6. Taken together, net gain of

*PTEN* (10q23) and loss of *FBXO9* (6p12) were exclusively observed in most of the cells in the metastatic LTL-220M subline in contrast to LTL-220N and LTL-221 sublines, suggesting this molecular signature could be used as a marker to identify the presence of such a subpopulation in the parental tissues.

Screening of cells in sections of parental xenografts of the non-metastatic LTL-220N and LTL-221N showed two copies each for *PTEN* (10q23), centromere 6 and *FBXO9* (6p12) as observed in the established tumor lines (Fig. 4E,F). However, the parental xenograft of the metastatic LTL-220M line showed heterogeneity in copy number for each of the genomic loci tested: (i) the majority of cells (60%) possessed two copies of *PTEN* (10q23), centromere 6 and *FBXO9* (6p12); (ii) a small population (~20%) possessed two copies of *PTEN*
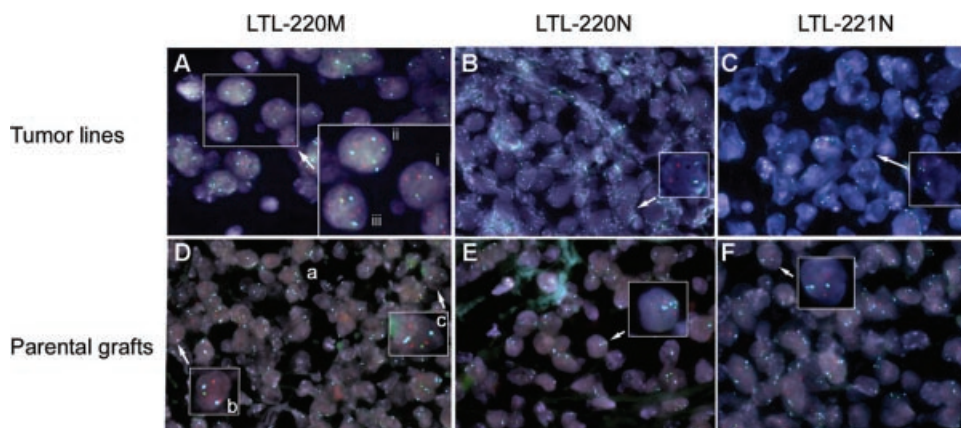
**Fig. 4.** FISH detection of I0q and 6p alterations in the LTL-220M, LTL-220N, LTL-22IN sublines and their parental (first-generation) grafts. **A**: The metastatic LTL-220M tumor line showed a net loss of FBXO9 (6pI2) and gain of PTEN (I0q23). Insets represent three detected clones: (i) gain of PTEN, loss of FBXO9, two copies of centromere 6; (ii) gain of PTEN, three copies of centromere 6, two copies of FBXO9; (iii) gain of PTEN, two copies of centromere 6, one copy of FBXO9. **B,C**: The non-metastatic LTL-220N and LTL-22IN sublines were consistently identified with two copies of PTEN, centromere 6 and FBXO9 per cell. **D**: The parental xenograft of the metastatic LTL-220M line showed heterogeneity in copy number for each of the genomic loci tested: (a) the majority of cells (60%) possessed two copies of PTEN (I0q23), centromere 6 and FBXO9 (6pI2); (b) a small population (∼20%) possessed two copies of PTEN (I0q23), centromere 6 and one copy of FBXO9 (6pI2); (c) the rest (∼20%) showed gain of PTEN (I0q23), two copies of centromere 6 and one copy of FBXO9 (6pI2) **E,F**: The parental xenografts of the non-metastatic LTL-220N and LTL-22IN showed two copies each for PTEN (I0q23), centromere 6 and FBXO9 (6pI2) as observed in the established tumor lines (PTEN: red; FBXO9: green; centromere 6: blue). [Color figure can be viewed in the online issue, which is available at wileyonlinelibrary.com.]

(10q23), centromere 6 and one copy of *FBXO9* (6p12); (iii) the rest (∼20%) showed gain of *PTEN* (10q23), two copies of centromere 6 and one copy of *FBXO9* (6p12) (Fig. 4D). This last subpopulation in the parental xenograft showed the same *PTEN*, centromere 6 and *FBXO9* copy number changes as the type (iii) subpopulation in the metastatic LTL-220M subline, indicative of metastatic potential.

## DISCUSSION

Tumor heterogeneity in both primary and metastatic prostate cancers is a major hurdle in elucidating the mechanisms of metastasis. To circumvent this obstacle and improve our understanding of prostate cancer metastasis, we developed multiple tumor tissue sublines from one patient's primary prostate cancer specimen. In our laboratory, many transplantable prostate cancer tumor lines have been developed using subrenal capsule xenografting in immuno-deficient mice [16,22]. Subrenal capsule xenografting allows for a very high engraftment rate (>90%) [17], in contrast to rates achieved when grafting tissues subcutaneously (take rates of 20–40%) [23–27]. The high engraftment rate is likely a result of high tissue perfusion of the kidney, providing superior nutrient supply for better graft survival and development of graft microvascularity [13,14,17–19]. This is especially important for minimizing loss of tumor subpopulations during grafting. Using the subrenal capsule grafting

methodology, many prostate cancer tumor lines were developed from primary prostate cancer tissues by our laboratory. In this study, the three sublines were generated from one patient's prostate cancer specimen, despite their significant differences in growth rate and karyotype (Fig. 3, Table I). This diversity is consistent with the widely accepted heterogeneous nature of prostate cancers. Importantly, the sublines also showed marked differences in local tissue invasiveness and metastatic ability as shown by an in vivo metastatic assay (Fig. 2). This provides functional evidence of the presence in the primary tumor of subpopulations with different metastatic potential.

SKY was instrumental in identifying chromosomal aberrations (gain of 10q and loss of 6p) present in the metastatic LTL-220M subline in contrast to the non-metastatic sublines. More importantly, FISH analysis confirmed the SKY findings and using the gain of 10q (i.e., *PTEN*) and loss of 6p (i.e., *FBXO9*) as a ''metastatic signature,'' we were able to specifically identify the metastatic LTL-220M subline cells. The small differences observed with the probes in the three LTL-220M subline subpopulations are probably a result of genomic instability. It should be noted that the *PTEN* and *FBXO9* probes were only used to identify cells with 10q gain and 6p loss for proof-of-hypothesis in this particular case. The gene copy number changes do not appear to be suitable as general markers of metastasis, since loss of the *PTEN* gene, rather than its gain, is usually observed in prostate cancer development and

metastasis [28]. In fact, no PTEN protein expression was detected in LTL-220M cells by immunohisto-chemistry in spite of *PTEN* copy number gain (Supplementary data), which is consistent with the reports of *PTEN* inactivation by epigenetic regulation or mutation in advanced prostate cancers [29,30]. Studies aimed at identifying metastatic markers may benefit from further studies with these and other paired patient-derived metastatic and non-metastatic tumor sublines at the RNA or protein level.

The small percentage of cancer cells in the parental tissues that were identified with the ''metastatic signature'' indicates that metastatic ability was associated with a minority rather than a majority of the cells at least in some primary tumors. This finding is consistent with the clonal selection hypothesis of metastasis proposed by other groups which used cultured mouse cell lines [31,32]. However, it is in contrast with a report that the metastatic potential of human tumors is encoded in the bulk of a primary tumor [12]. In that study, pools of cancer cells were analyzed with an array-based method, involving a signature composed of 17 genes that could not distinguish cells with full metastatic ability from cells that responded only partially to the gene probing. As a result more cells could have been identified as being metastatic than were actually present in the primary tumor. In the present study, the finding that metastatic potential is associated with a subpopulation in the primary tumor was made by screening of individual cells with a signature that had been successfully used to distinguish cells with metastatic ability as shown by an in vivo assay. While the present study indicates that metastatic potential of cells in a primary tumor may be associated with a small subpopulation, it is recognized that in some cases primary tumors may contain a large subpopulation of metastatic cells due to the fast outgrowth of a metastatic clone. In any case, it is essential to establish signatures for specific identification of cells with metastatic potential.

The metastatic and non-metastatic prostate cancer sublines used in the present study were established from one patient's fresh primary tumor tissue which highly favored retention of properties of the original cancer, using identical experimental conditions (e.g., micro-environment). As such they are very similar in genetic background. Some genetic differences that they do display are likely related to metastatic ability. In view of this, the sublines could provide useful tools for identifying metastasis-associated genes via, for example, comparative gene expression analysis. It is likely that genes, found to be differentially expressed in metastatic and non-metastatic prostate cancer sublines, will include some with critical roles in metastasis. Such genes and/or their products could serve as potential targets for therapy of metastatic prostate cancer.

## REFERENCES

1. Jemal A, Ward E, Hao Y, Thun M. Trends in the leading causes of death in the United States, 1970–2002. JAMA 2005;294(10):1255–1259.

2. Fidler IJ. The pathogenesis of cancer metastasis: The 'seed and soil' hypothesis revisited. Nat Rev Cancer 2003;3(6):453–458.

3. Gupta GP, Massague J. Cancer metastasis: Building a framework. Cell 2006;127(4):679–695.

4. Arora R, Koch MO, Eble JN, Ulbright TM, Li L, Cheng L. Heterogeneity of Gleason grade in multifocal adenocarcinoma of the prostate. Cancer 2004;100(11):2362–2366.

5. Bostwick DG, Shan A, Qian J, Darson M, Maihle NJ, Jenkins RB, Cheng L. Independent origin of multiple foci of prostatic intraepithelial neoplasia: Comparison with matched foci of prostate carcinoma. Cancer 1998;83(9):1995–2002.

6. Ruijter ET, van de Kaa CA, Schalken JA, Debruyne FM, Ruiter DJ. Histological grade heterogeneity in multifocal prostate cancer. Biological and clinical implications. J Pathol 1996;180(3):295–299.

7. Wise AM, Stamey TA, McNeal JE, Clayton JL. Morphologic and clinical significance of multifocal prostate cancers in radical prostatectomy specimens. Urology 2002;60(2):264–269.

8. Ruijter ET, Miller GJ, van de Kaa CA, van Bokhoven A, Bussemakers MJ, Debruyne FM, Ruiter DJ, Schalken JA. Molecular analysis of multifocal prostate cancer lesions. J Pathol 1999;188(3):271–277.

9. Cheng L, Song SY, Pretlow TG, Abdul-Karim FW, Kung HJ, Dawson DV, Park WS, Moon YW, Tsai ML, Linehan WM, Emmert-Buck MR, Liotta LA, Zhuang Z. Evidence of independent origin of multiple tumors from patients with prostate cancer. J Natl Cancer Inst 1998;90(3):233–237.

10. Barry M, Perner S, Demichelis F, Rubin MA. TMPRSS2–ERG fusion heterogeneity in multifocal prostate cancer: Clinical and biologic implications. Urology 2007;70(4):630–633.

11. Mehra R, Han B, Tomlins SA, Wang L, Menon A, Wasco MJ, Shen R, Montie JE, Chinnaiyan AM, Shah RB. Heterogeneity of TMPRSS2 gene rearrangements in multifocal prostate adenocarcinoma: Molecular evidence for an independent group of diseases. Cancer Res 2007;67(17):7991–7995.

12. Ramaswamy S, Ross KN, Lander ES, Golub TR. A molecular signature of metastasis in primary solid tumors. Nat Genet 2003;33(1):49–54.

13. Sharpless NE, Depinho RA. The mighty mouse: Genetically engineered mouse models in cancer drug development. Nat Rev Drug Discov 2006;5(9):741–754.

14. Voskoglou-Nomikos T, Pater JL, Seymour L. Clinical predictive value of the in vitro cell line, human xenograft, and mouse allograft preclinical cancer models. Clin Cancer Res 2003;9(11):4227–4239.

15. Fidler IJ. Critical determinants of metastasis. Semin Cancer Biol 2002;12(2):89–96.

16. Wang Y, Xue H, Cutz JC, Bayani J, Mawji NR, Chen WG, Goetz LJ, Hayward SW, Sadar MD, Gilks CB, Gout PW, Squire JA, Cunha GR, Wang YZ. An orthotopic metastatic prostate cancer model in SCID mice via grafting of a transplantable human prostate tumor line. Lab Invest 2005;85(11):1392–1404.

17. Wang Y, Revelo MP, Sudilovsky D, Cao M, Chen WG, Goetz L, Xue H, Sadar M, Shappell SB, Cunha GR, Hayward SW. Development and characterization of efficient xenograft models for benign and malignant human prostate tissue. Prostate 2005; 64(2):149–159.

18. Lee CH, Xue H, Sutcliffe M, Gout PW, Huntsman DG, Miller DM, Gilks CB, Wang YZ. Establishment of subrenal capsule xenografts of primary human ovarian tumors in SCID mice: Potential models. Gynecol Oncol 2005;96(1):48–55.

19. Cutz JC, Guan J, Bayani J, Yoshimoto M, Xue H, Sutcliffe M, English J, Flint J, LeRiche J, Yee J, Squire JA, Gout PW, Lam S, Wang YZ. Establishment in severe combined immunodeficiency mice of subrenal capsule xenografts and transplantable tumor lines from a variety of primary human lung cancers: Potential models for studying tumor progression-related changes. Clin Cancer Res 2006;12(13):4043–4054.

20. Bayani J, Squire JA. Preparation of cytogenetic specimens from tissue samples. In: Bonifacino JS, editor. Current Protocols in Cell Biology, Suppl 23. New York: John Wiley & Sons, Inc.; 2004. 22.2.1–22.2.15.

21. Yoshimoto M, Cutz JC, Nuin PA, Joshua AM, Bayani J, Evans AJ, Zielenska M, Squire JA. Interphase FISH analysis of PTEN in histologic sections shows genomic deletions in 68% of primary prostate cancer and 23% of high-grade prostatic intra-epithelial neoplasias. Cancer Genet Cytogenet 2006;169(2):128–137.

22. Lin D, Watahiki A, Bayani J, Zhang F, Liu L, Ling V, Sadar MD, English J, Fazli L, So A, Gout PW, Gleave M, Squire JA, Wang YZ. ASAP1, a gene at 8q24, is associated with prostate cancer metastasis. Cancer Res 2008;68(11):4352–4359.

23. Perez-Soler R, Kemp B, Wu QP, Mao L, Gomez J, Zeleniuch-Jacquotte A, Yee H, Lee JS, Jagirdar J, Ling YH. Response and determinants of sensitivity to paclitaxel in human non-small cell lung cancer tumors heterotransplanted in nude mice. Clin Cancer Res 2000;6(12):4932–4938.

24. Johnson JR, Hammond WG, Benfield JR, Tesluk H. Successful xenotransplantation of human lung cancer correlates with the metastatic phenotype. Ann Thorac Surg 1995;60(1):32–36; discussion 36–37.

25. Fichtner I, Rolff J, Soong R, Hoffmann J, Hammer S, Sommer A, Becker M, Merk J. Establishment of patient-derived non-small cell lung cancer xenografts as models for the identification of predictive biomarkers. Clin Cancer Res 2008;14(20):6456–6468.

26. Mattern J, Jager S, Sonka J, Wayss K, Volm M. Growth of human bronchial carcinomas in nude mice. Br J Cancer 1985;51(2):195–200.

27. Merk J, Rolff J, Becker M, Leschber G, Fichtner I. Patient-derived xenografts of non-small-cell lung cancer: A pre-clinical model to evaluate adjuvant chemotherapy? Eur J Cardiothorac Surg 2009;36(3):454–459.

28. Gray IC, Stewart LM, Phillips SM, Hamilton JA, Gray NE, Watson GJ, Spurr NK, Snary D. Mutation and expression analysis of the putative prostate tumour-suppressor gene PTEN. Br J Cancer 1998;78(10):1296–1300.

29. Li J, Yen C, Liaw D, Podsypanina K, Bose S, Wang SI, Puc J, Miliaresis C, Rodgers L, McCombie R, Bigner SH, Giovanella BC, Ittmann M, Tycko B, Hibshoosh H, Wigler MH, Parsons R. PTEN, a putative protein tyrosine phosphatase gene mutated in human brain, breast, and prostate cancer. Science 1997; 275(5308):1943–1947.

30. Whang YE, Wu X, Suzuki H, Reiter RE, Tran C, Vessella RL, Said JW, Isaacs WB, Sawyers CL. Inactivation of the tumor suppressor PTEN/MMAC1 in advanced human prostate cancer through loss of expression. Proc Natl Acad Sci USA 1998;95(9):5246–5250.

31. Fidler IJ, Kripke ML. Metastasis results from preexisting variant cells within a malignant tumor. Science 1977;197(4306):893–895.

32. Fidler IJ, Talmadge JE. Evidence that intravenously derived murine pulmonary melanoma metastases can originate from the expansion of a single tumor cell. Cancer Res 1986;46(10):5167–5171.